



An Experimental Study of Locally Assembled Vacuum Chamber and Estimation of Sample Porosities from Various Formations, Northern Iraq

Bafren Kamil Raof , Khabat Mohammed Ahmed , Rand Mohammed Othman 

Department of Petroleum and Energy, College of Engineering, University of Sulaimani Polytechnic, Iraq

Received: 13 Sep. 2024 Received in revised form: 10 Oct. 2024 Accepted: 15 Oct. 2024

Final Proofreading: 30 Oct. 2024 Available online: 25 Feb. 2025

ABSTRACT

In this study, the porosity measurement of fourteen outcrop samples from different locations is examined using an in-house vacuum chamber. The vacuum chamber is tested for any leak to secure the experiment's integrity. To meet the process development required, part of the samples was tested in a more sophisticated device to provide well-aimed results and decrease the margin of error where B (1,2) and S5 were measured using a nitrogen porosimeter to attain further accuracy and reliability and compare the results to a saturation method. Both measurements of porosity can provide insights into the outcome of the constructed porosimeter. Afterward, the water saturation for the remaining samples was commenced and the results of the last nine samples in crude oil are compared. Notably, S6 has a porosity of (9.89 %) by water imbibition and (3.46 %) by crude oil imbibition which suggests that the S6 sample is strongly water-wet rock. S7 and S13 have a porosity increase of (1.46 %) and (3.84 %), respectively in crude oil saturation and it can be an indication of oil-wet rock. The objective of this research is to design and assemble an affordable porosimeter and evaluate through porosity measurement the samples from various formations.

Keywords: Porosity, Water and crude oil saturation, Wettability, Vacuum chamber

Name: Bafren kamil Raof

E-mail: bafrenkamil@spu.edu.iq



©2025 THIS IS AN OPEN ACCESS ARTICLE UNDER THE CC BY LICENSE
<http://creativecommons.org/licenses/by/4.0/>

دراسة تجريبية لجهاز تفرغ وتقدير مسامية نماذج من طبقات مختلفة، شمال العراق

بفرين كامل رؤوف، خبات محمد احمد، رند محمد عثمان

قسم النفط والطاقة، كلية الهندسة، جامعة السليمانية التقنية، العراق

الملخص

في هذه الدراسة يتم قياس المسامية والمعانة لأربعة عشر نموذجاً من مواقع مختلفة عن طريق استعمال جهاز تفرغ محلي. جهاز التفرغ يتم فحصه لوجود اي تسريب فيه لضمان صحة التجربة. لأجل الاستمرار المطلوب، تم فحص قسم من النماذج بجهاز متطور لتقليل نسبة الخطأ والحصول على نتائج محكمة تم قياس B (1,2) و S5 بجهاز قياس المسامية النيتروجيني ومقارنة النتائج للتشبع المائي. كلا القياسين يزودان نظرة على مخرجات الجهاز المصنوع. بعد فحوصات التشبع المائي، تتم مقارنة النتائج بالتشبع النفطي للنماذج التسعة المتبقية. الجدير بالذكر ان نموذج S6 له مسامية (9.89 %) عن طريق التشبع المائي و (3.46 %) عن طريق بالتشبع النفطي وهذا يحتمل بسبب التبليبية المائية العالية. شهدت مسامية S7 و S13 زيادة بنسبة (1.46 %) و (3.84 %) على التوالي في النفط الخام ويحتمل ان يكونان ذوا تبلل نفطي او مختلط. هدف الدراسة هو تصميم وتجميع جهاز قياس مسامية بكلفة معقولة وتقييمه عن طريق قياس المسامية من طبقات مختلفة.

INTRODUCTION

After decades of research and development, a series of devices have been designed to establish the foundation for a deeper comprehension of the structure of various formations from petrophysical properties such as the porosity, permeability saturation, etc., which on the one hand improve the result and efficiency of well completion, perforation forecasting consequently prolonging the service life of reservoir. From the viewpoint of petroleum industry developers, the porosity of a rock is a measure of the storage capacity (pore volume) that is capable of holding fluids, providing a flow path for oil and gas ⁽¹⁾. Hence, the rock looks solid to our eyes, but in reality, consists of a network of miniature openings as revealed by a microscopic examination ⁽²⁾. It controls the storage, connectivity, and transport properties of pore networks, as well as the relationships between the properties of individual minerals and the bulk properties of the rock ⁽³⁾. The results of the correlations between the petrophysical analysis, the Porosity Image Analysis (PIA) method, and core analysis reveal good correlations with negligible standard errors ⁽⁴⁾.

Overall porosimeter technology could be divided into several traditional categories ⁽⁵⁾. However, new edge techniques are employed to evaluate the porosity of an oil well core such as Nuclear Magnetic Resonance (NMR) by detecting the response of hydrogen nuclei trapped in pores to a magnetic field ⁽⁶⁾. Digital Rock Physics (DRP) by employing X-ray computed tomography and focused ion beam scanning microscopy to create a detailed digital model without physically altering the sample one ⁽⁷⁾ with high precision provides high precision and small random error of the obtained results in the repeatability conditions is the helium porosimeter ⁽⁸⁾. However, the results may vary for the same formation as the grains undergo irreversible deformation due to dissolution-recrystallization, fracture, or plastic flow, and all such decreases in porosity ⁽⁹⁾. Porosity is also controlled by mechanical processes, such as stress compaction, plastic deformation, brittle deformation, fracture evolution, etc., and geochemical processes, such as dissolution, precipitation, volume reductions concomitant upon

mineralogical changes, etc.⁽¹⁰⁾. The most important role of rock characteristics during saturation is the wettability of the rocks, for example, if water floods into a water-wet rock, the flow will be different from the case of an oil-wet rock. This is due to the low mobility of water in a water-wet rock as water wants to stick to the surface while the oil will be expelled out easily. Therefore, wettability affects the flow in porous media ⁽¹¹⁾. However, the wettability may be altered in comparison to the initial one, and the reasons may be rendered to ion exchange of the environment, mineral dissolution, and salt precipitation. Various studies have been conducted on the effect of weathering on the chemical and mechanical properties of surface samples ⁽¹²⁾. examined exposed geological formations and found that the samples were suffering innumerable factors that may alter their properties. The temperature fluctuation from mid-day to night and being subjected to high wind or rain lead to mechanical stress, changing the surface roughness presented that weathering causes changes in cohesion, hydraulic properties, and the appearance of microstructures that are filled with clay from chemical and physical weathering ⁽¹³⁾ investigated the surface change that occurs through repeated cycles of drying and wetting. A conclusion was reached that the wettability, different pore structure, and surface chemistry have been altered ⁽¹⁴⁾. The Fluid in contact with the surface results in altered wettability due to chemical interactions with the minerals ^(15, 16) or the adsorption of polar components from the oil onto the rock surface^(17, 18) showed that the salt concentration in an aqueous and pH level affects the mineral surface charge, resulting in an altered wettability integrating both sandstone and carbonate sufficiently contributes to reservoir characterization. Sedimentary rocks, of which almost all hydrocarbon reserves are made⁽¹⁹⁾. Typically, carbonate porosity varies from (1 to 35 %), average porosity in dolomite formations is (10 %) and in limestone formations is (12 %) ⁽²⁰⁾. The main objective of this study is to use an in-house

porosimeter that operates efficiently and easily and correlates the results to a nitrogen porosimeter for different formations.

MATERIAL AND METHOD

Specimens are extracted from outcrops from different locations in the Northern Iraq. Before any petrophysical measurement, such as porosity, permeability, and so on, cleaning the samples after preparing the sample plugs is necessary based on the location of the core and existing impurities. Soxhlet distillation extraction utilizing dichloromethane can remove impurities and hydrocarbons from the samples under solvent vaporization and condensation and this is the standard procedure in the Kurdistan Strategic Research Center-Sulaymaniyah. The apparatus is designed for regular samples, so in the case of irregular samples, they are extracted after taking off the surface layer by utilizing a hammer. brushing, and washing in pure distillate water, afterward, (100 %) ethanol is used to remove access-grain fragments and fines, and dissolve salt in an attempt to attain a surface as chemically pure as possible. From the review of methods for measuring the porosity of a sample plug, the water saturation is the one that provides a glance at rock types, porosity, wettability and operates at ease. To carry on with the experiment, a porosimeter was assembled with simple parts locally. The advantages of being economical, leakage-free, and time-saving are our goal at this point. As an improved point, we inquired about more accurate values for the pore volume (V_p) that were attained from a sophisticated porosimeter analysis measuring the first five samples. Such improvement can minimize the errors of the original method and generate a better analysis of the results. Additionally, the pore volume measurement from the water saturation method is adapted for all fourteen samples. A saturation with crude oil took place in the vacuum chamber to distinguish between the imbibition of both the crude oil and water for the last nine samples (S6 to S14).

Assembly and Leakage Test

The designing process started with a vacuum chamber, a vessel that is used in scientific laboratories to carry out the task of evacuating and creating conditions close to those of space. Pyrex glass is borosilicate glass that is highly resistant to thermal shock, and has an appropriate thickness of (10 mm) that prevents damage during evacuating air. To prevent leaking between two objects, silicone sealant is fixed as a gasket which offers a reliable and flexible seal to maintain a vacuum between the glass vessel and the lid. The lid was used as a cap for the Pyrex glass, epoxy resin was molded and used. Prior to the epoxy curing a (2 inch) nozzle was placed to prevent any leakage during vacuuming. The nozzle sucks air of the chamber and accordingly is connected to a T shape distributor at two ball valves at the end of both of them. The first valve (roughing valve) is connected to the compressor through a roughing line which is connected to a quick release at the air vacuum portal in the compressor ZA-5050 air compressor is utilized by converting it to a vacuum pump and replacing the air filter with attach the coupling to the air hose. The vent valve is used for restoring the atmospheric pressure, so it allows the air to flow into the vacuum chamber and equalizes the pressure inside the chamber with external atmospheric pressure, this equalization of pressure allows the lid to be detached effortlessly. Methods can be applied to leaking tests such as (sniffing)⁽²¹⁾. The right valve is connected to the Helium container, the saturation apparatus is pressurized, a gas detector is set close by, and a certain amount of leak was witnessed. However, their exact locations were unidentified. A visual leak test was attained to locate the exact leakage point by vacuum air from the vessel, prior to the vacuum apply a soapy solution, turn on the compressor to evacuate air from the chamber and create a vacuum, and observe all areas where the solution is applied and look for bubbles which indicate a leak of air, in case of no leaking the assembly is ready for the experiment. The chamber

consists of the following parts as can be seen in [Figure \(1\)](#):

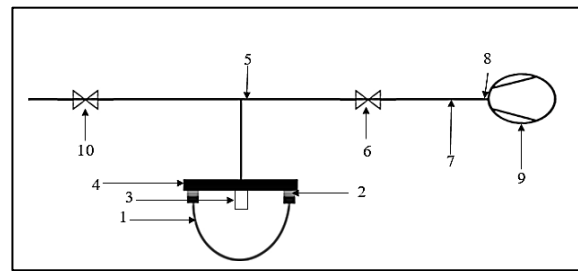


Fig. 1: In-house Porosimeter, 1-Vacuum Chamber, 2-Gasket, 3- Nozzle, 4-lid, 5-T shape distruster, 6-Roughing valve, 7-Roughing line, 8-quick released coupling, 9-Air compressor 10-Vent valve.

Measurements and Preparations

From outcrops, irregular specimens were extracted ([Table \(1\)](#) and [Figure \(2\)](#)). Each specimen includes different properties and is obtained from various locations with the intent to ensure the examination of a wider range of specimens. Only five specimens were tested in a gas porosimeter for evaluation and comparison purposes, thus they were cut into a cylinder shape, their dimensions were measured using Vernier clippers as tabulated in [Table \(2\)](#). Both ends of them are cut and polished further and later being cut and trimmed. For most porosity analysis tests, the samples must be initially cleaned and dried to remove water, as well as, mud filtrate and wettability contaminants then dried using ventilation first and then put in an oven at (50 °C) for a minimum of (24 hours). Additionally, to the five cylindrical samples of the study, nine irregular different samples were prepared. As sandstone samples are frequently fragile, have large grain and pore sizes, and do not produce smooth surfaced right cylinders when plugs are drilled and accurate, bulk volume determination becomes difficult. Straightforward measurement with Vernier calipers is not possible and Archimedes method (liquid displacement method) has to be used ⁽²²⁾. The buoyant force acting on the submerged sample is measured. This force is equal to the weight of the fluid displaced by the sample, as per Archimedes' principle. By measuring the volume of fluid displaced, the sample's bulk volume is determined,

including both the solid matrix and the pore space. The most proper fluid to be used is one with no reaction to the sample such as mercury. However, it was not available so the alternative is water. The dry weight is recorded and to prevent the water from

invading the pores it was covered with pre-weighted plastic film and subtracted from the total bulk volume after water displacement. The fact that the samples are outcrop samples and have been in the presence of moisture after the measurement.

Table 1: The location of the samples.

Sample	Location	Coordinate	Rock type	Lithology
B1-1	Azmar-Sulaymaniyah	(35.5831944, 45.4945000)	Limestone	Balmbo
B1-2	Azmar-Sulaymaniyah	(35.5831944, 45.4945000)	Limestone	Balmbo
B2-1	Azmar-Sulaymaniyah	(35.5867778, 45.4937500)	Limestone	Balmbo
B2-2	Azmar-Sulaymaniyah	(35.5867778, 45.4937500)	Limestone	Balmbo
S5	Qader karam-Sulaymaniyah	(35.1366190, 44.8251310)	Sandstone	Upper Fars
S6	Kalar-Sulaymaniyah	(34.6574311, 45.4063781)	Sandstone	Upper Fars
S7	Sitak-Sulaymaniyah	(35.6342796, 45.4833931)	Sandstone	Tanjaro
S8	Biara-Sulaymaniyah	(35.2136202, 46.1324548)	Limestone	Qulqula
S9	Arbat-Sulaymaniyah	(35.4512654, 45.4982844)	Sandstone	Tanjiro
S10	Chamchamal-Sulaymaniyah	(35.4833921, 44.8664352)	Limestone	Upper Bakhtiari
S11	Khalo Baziani-Karkuk	(35.4215700, 44.6354500)	Limestone	Ana
S12	Chamchamal-Sulaymaniyah	(35.6136814, 44.8016962)	Sandstone	Upper Fars
S13	Kalar-Sulaymaniyah	(34.6574311, 45.4063781)	Sandstone	Upper Fars
S14	Soran-Erbil	(36.6475556, 44.5683333)	Sandstone	Walash

• The samples (B1 to B2) are located within Azmar Mountain, Northeastern Sulaymaniyah city with the coordinates mentioned previously. There are nearly (500 m) between the two samples (B1, B2). The anticline is about (43 Km) in length. The core of this anticline is composed of early Cretaceous rocks of the Balmbo Formation that crop out along the Sulaymaniyah Azmar main road⁽²³⁾. This section is in the Imbricated Zone characterized by the presence of various structural features and is composed of fine-grained limestone, marls, or friable papery shales of Berriasian to Berrmeain age⁽²⁴⁾. As⁽²⁵⁾ stated that the formation is rich in radiolarian, planktonic foraminifera, and ostracod carapace, with rare occurrence of sponge spicules. In the northern flank of the Azmar anticline and toward the northeast, the basal facies of the Balambo Formation progressively change into well-bedded hard limestone intercalated with thin marly layers. The studied sections comprise sedimentary sequences of the Neo-Tethys Sea which have been affected by the collision of the Arabian and Iranian plates. The samples S5, S6, S12, and S13 are from the Upper Fs Formation are taken from Qadir

Karam, Chamchal, and Kalar. The Upper Miocene Inaja (Upper Fars) Formation exists in Iraq widely; it also extends into northern Syria, Turkey, and over large areas in southern Iran, it is described as subcontinental to continental coarse and medium-grained carbonate-rich sandstone alternating with brownish red siltstones, mudstones, and marls with rare freshwater limestone⁽²⁶⁾. The reference sample S5 is located in the Kormor area, southwest Sulaymaniyah city. The area is (35 Km) long and (5 Km) wide and consists of an asymmetrical anticline covered with a thick layer of Injanah (Upper Fars) Formation.

• The samples S7 and S9 are from the Tanjro Formation. Tanjero Formation is an Upper Cretaceous (Campanian-Maastrichtian) unit, which crops out within the Imbricated and High Folded Zones in Northeastern Iraq⁽²⁷⁾. The down-tip extension of this surface, with associated conglomerate, reaches the middle part of Sharazoor, the typical lithology of Tanjero Formation consists of these wedges and the slope fans (alternation sandstone and shale). The wedge is conglomerate-rich in the proximal area, which is represented by

(500 m) of Kato conglomerate. at the foothill of Azmar and Goizha anticlines (28).

- Sample S8 is extracted from the Qulqula Formation. Qulqula Formation represents a stratigraphic unit from the Qulqula Group, which is divided into two formations; Qulqula radiolarian and Qulqula conglomerate formations. Qulqula Formation as described in its type locality consists of alternating chert, shale, and siliceous limestone rocks (29).
- Sample S10: is the limestone from the Upper Bakhtiari Formation found in the Chamchamal area which indicates the shallow marine depositional environment and is characteristic of the Pliocene Pleistocene age.(30). The Upper Bakhtiari is well known for its polymictic conglomerate in Iran, Iraq and Turkey. According to the recent study the Upper Bakhtiari Formation composed of mixture of gravels and boulders of cherts, limestones and igneous clasts. This limestone, containing mainly calcium carbonate, presents tectonic and sedimentary characteristics of the Zagros Fold-Thrust Belt. A succession of limestone

conglomerate that belonging to the aforementioned formation (31).

- The sample S11 is taken from a limestone of the Ana Formation, a complex of backreef/reef/forereef basinal units (32).
- S14 belongs to the Walsh Group, according to(33) the volcanic rock of the Walsh- Naopurdan volcano- sedimentary group are representative of magmatic series. Walsh- Naopurdan Group, which contains an extended distribution of ultramafic, mafic and volcano- sedimentary rocks, includes a wide variety of mineral resources. In the intermountain basin the flysch facies (sandstone and shale of Walsh- Naoperdan group are deposited during Middle Eocene (3). The sandstones of the Walsh Group are of two basic types. The dominant type is litharenite. It is generally noticed in the lower and middle parts of the lower unit. It ranges from medium to coarse-grained in size. Grains are dominated by lithic fragments of carbonate (limestone and dolostone), chert, and igneous origin (34).

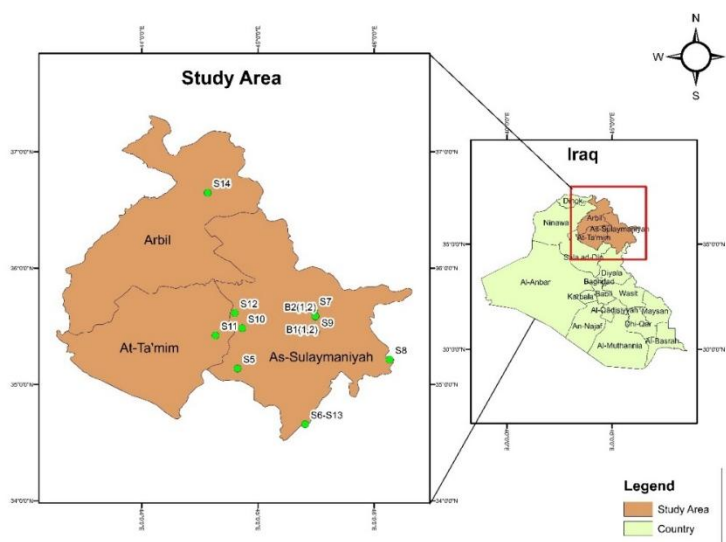


Fig. 2: The location of referred samples.

Gas Expansion Porosimeter

Porosity can be measured using various methods for instance, the computed tomography method which is an advanced imaging technology to create 3D models of the core and enables precise measurement of porosity. Unfortunately, computed tomography is

not available in the universities of Kurdistan region. The other methods are imbibition, water evaporation, mercury intrusion, and gas expansion. The mercury intrusion method is not popular because of environmental regulations and policies. Water evaporation is rarely being used because in

some cases, reaction might happen between the grain material and injected water. The gas expansion method is widely used in the oil and gas industries because gas has small molecules that can easily penetrate through the pore throats and no reaction happens between grains and injected gas. In addition, the selected core plugs can be used for further studies such as permeability, water saturation, and other special core analyses. The OFITE model 350 Core Porosimeter was used for the measurement. This method relies on the ideal gas law, or rather Boyle's law. The rock is sealed in a container of known volume V_1 at atmospheric pressure P_1 . This container is attached by a valve to another container of known volume, V_2 , containing gas at a known pressure, P_2 . When the valve that connects the two volumes is opened slowly so that the system remains isothermal, the gas pressure in the two volumes equalizes to P_3 . The value of the equilibrium pressure can be used to calculate the volume of grains in the rock V_s . Boyle's Law states

that the pressure times the volume of a system is constant. It is insensitive to mineralogy and leaves the sample available for further petrophysical tests accordingly ⁽¹⁾. Thus, samples 1 to 5 are considered as reference samples for our experiment. The following equations are employed to calculate the parameters in [Table 2](#).

$$\text{Sample bulk volume (cc): } V_B = \pi \frac{D^2}{4} L \quad \dots (1)$$

$$\text{Sample chamber volume (cc): } V_3 = V_1 \frac{P_1}{P_2} \quad \dots (2)$$

$$\text{Sample grain volume (cc): } V_G = V_2 - V_3 \quad \dots (3)$$

$$\text{Sample pore volume (cc): } V_p = V_B - V_G \quad \dots (4)$$

$$\text{Porosity (\%): } \Phi = \frac{V_p}{V_B} \times 100\% \quad \dots (5)$$

Where D , L represent the diameter and the length of the sample respectively, V_1 , V_2 represent the fixed volume and chamber volume after the gas expansion respectively, and P_1 , P_2 represent the initial pressure and the equilibrium pressure after the gas expansion respectively.

Table 2: Samples of geometrical and geophysical properties.

Sample	D (cm)	L (cm)	V ₁ (cc)	V ₂ (cc)	P ₁ (psi)	P ₂ (psi)	V _B	V _p	V _G	Φ
B1-1	3.75	4.20	58.64	161.18	180.9	88.5	47.15	5.83	41.32	12.38
B1-2	3.75	4.66	58.64	161.18	180.8	93.3	52.32	4.77	47.55	9.21
B2-1	3.75	4.35	58.64	161.18	180.9	90.0	48.84	5.53	43.31	11.31
B2-2	3.75	4.62	58.64	161.18	180.8	91.5	51.87	6.56	45.31	12.64
S5	3.78	3.66	58.64	161.18	180.0	83.0	41.09	7.08	34.01	17.23

According to the study conducted by Albeyati ⁽³⁴⁾ in the case of very small samples petrophysical properties, porosity and permeability could be measured from Weber (1987) in the case if having very small samples.

Pore Volume measurement by imbibition method

There is not a solely ASTM for imbibition method using water saturation but similar porosity measurement can be applied such as the D4404-18 Standard Test Method for Determination of Pore Volume and Pore Volume Distribution of Soil and Rock by Mercury Intrusion Porosimeter ⁽³⁵⁾. The previously tested samples (1-5) are considered as

reference samples for the experiment, the saturation method is applied to them in the vacuum chamber to mark the difference between the two measurements. Furthermore, an extra nine irregular samples were fetched from various locations to test the device. The surface exposed sample was dried to remove any excess water utilizing a vacuum oven. Recording the dry weight and recording repetitive readings until stable saturation is reached. The saturated weight difference between readings has decreased obviously with time. Taping and surface drying of the sample was essential to eliminate extra water. Time is crucial to saturate and weigh the samples Therefore, a time-lapse is set for each

measurement to be (5 minutes) between each vacuum. In the fourth trial same reading as the prior one was obtained, the third reading can be observed in [Table \(3\)](#). However, some samples had the same weight in the third trial and that is connected to the permeability of the sample and pore-scale distribution ⁽¹⁾. The test and weight measurements continued until there was no appreciable change in the weight readings between the two successive steps. It required four measurements for most samples. Noteworthy that due to the fragile composition of samples, a slight fissure was perceived, emanating a lower dry weight for the crude oil. The procedure is repeated for an extended duration between each measurement.

RESULTS AND DISCUSSION

Water saturation measurement

The porosity of the rock samples is measured using the water imbibition method, in which the rock is completely saturated with water, water density is (0.955 g/m³). The tests are continued until no more water is absorbed, and then the stabilized wet weights are obtained, the results are tabulated below through the use of the following equations:

water weight (gm):

$$W_{water} = W_{saturated} - W_{dry} \quad \dots (6)$$

$$\text{Sample pore volume (cc): } V_p = \frac{W_{water}}{\rho_{water}} \quad \dots (7)$$

For the irregular samples displacement method was used to find their bulk volume.

Table 3: Porosity from water imbibition method.

Rock samples	VB (Cm ³)	Dry weight (gm)	1 st wet Weight (gm)	2 nd wet weight (gm)	last wet weight (gm)	Porosity (%)
B1-1	46.15	116.69	117.11	117.54	118.53	4.17
B1-2	52.32	133.86	134.07	134.14	135.58	3.44
B2-1	48.84	124.27	124.63	124.77	125.26	2.12
B2-2	51.87	129.53	130.05	130.35	130.35	1.65
S5	39.00	98.72	101.14	101.23	101.23	6.86
S6	43.00	108.03	112.09	110.43	112.09	9.89
S7	78.00	194.43	197.80	198.40	198.55	5.53
S8	125.00	322.80	323.49	324.41	325.99	2.67
S9	170.00	424.51	426.01	427.63	428.59	2.51
S10	123.50	332.74	332.86	332.87	332.87	0.11
S11	109.00	289.15	289.30	289.45	289.45	0.29
S12	106.00	263.71	269.55	271.16	271.56	7.76
S13	91.00	217.63	220.65	221.80	222.38	5.46
S14	196.00	518.54	519.95	522.32	382.04	2.02

The samples exhibit different porosity readings although mostly are extracted from the same formation and outcrops. For example, the sandstone from Upper Fars Formation exhibits fairly good readings ranging from the highest porosity for S6 at (9.89 %) to the lowest for S13 at (5.46 %). The Balmo Formation samples (B1, B2) showed variation in their porosity and it is considered due to mineral dissolution, weathering, or scaling consequently affecting the permeability of the samples. The Tanjaro Formation samples (S7, S9) exhibited a relatively medium porosity considering that water imbibition is carried on the samples. Both

S14 from Walsh Group and S8 from Qulqula Formation porosities are very poor. At the same time, S10 and S11 hold the merest ratio, which are mostly considered impermeable layers and possess poor pore structure and distribution reflected in the saturation process.

Nitrogen porosity measurement and water imbibition porosity comparison

The results from the Nitrogen porosimeter for the reference samples are compared to the water saturation in [Table \(4\)](#), higher porosity measurement is obtained from the nitrogen porosimeter and the reasons are attributed firstly to

the nitrogen's ability to measure micro-sized pores in a more efficient way considering its high compressibility aids the flowability into pores. Secondly, water is denser and has higher surface tension. The other reason relies on the sample surface interactions with different fluids, as some may rebel against water and the fluid cannot easily flow into the pores. The statistical analysis calculates a correlation between both porosity measurements to describe the strength and direction of the linear relationship between two quantitative paired variables such as Pearson's correlation coefficient (2). The Pearson correlation coefficient is (0.71) calculated from equation (8). It indicates that there is a positive correlation between the two measurements. After a linear regression calculation

y represents the nitrogen porosity measurement suggesting that for every porosity measurement through the water imbibition method resulting in nil reading, there will be a 9.43% higher rate in nitrogen porosity as seen in Figure 3. The R-squared value represents about (55%) of the variability in the Nitrogen porosimeter measurement and is considered a moderate value.

$$r = \frac{\sum((x_i - \bar{x})(y_i - \bar{y}))}{\sqrt{\sum(x_i - \bar{x})^2 + \sum(y_i - \bar{y})^2}} \quad \dots (8)$$

Where r is the Pearson coefficient, x_i is the porosity measurement using the nitrogen porosimeter, \bar{x} is the mean porosity value using nitrogen porosimeter, y_i is the porosity measurement using the water saturation method, and \bar{y} is the mean porosity value using water saturation method.

Table 4: Comparison between nitrogen porosimeter and water saturation.

Sample	V3 (cm ³)	VB (Cm ³)	VG (cm ³)	Vp (cm ³)	Porosity N%	Porosity H ₂ O %	Difference
B1-1	119.86	47.15	41.32	5.83	12.38	4.17	8.21
B1-2	113.63	52.32	47.55	4.77	9.12	3.44	5.68
B2-1	117.87	48.84	43.31	5.53	11.31	2.12	9.19
B2-2	115.87	51.87	45.31	6.56	12.64	1.65	10.81
S5	127.17	41.09	34.01	7.00	17.23	6.86	10.37

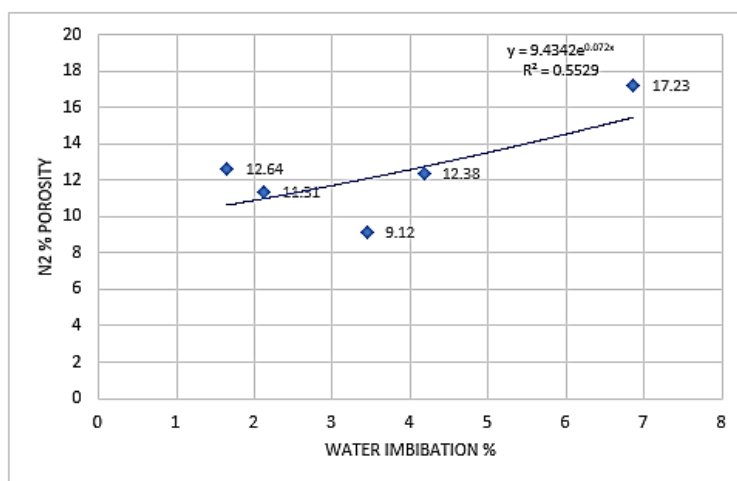


Fig 3: Porosity measurement comparison between N2 porosimeter and Water imbibition.

Furthermore, a nearby predicated result is obtained after the comparison between Pearson's correlation and the data in Table 4, reducing the error margin. For instance, following the application of the correlation on samples B1-1, B1-2, B2-1, B2-2, and S5, the results yield (13.60, 12.87, 11.55, 11.08, and

16.29 %), respectively. It is anticipated that the B1-2 sample should have demonstrated a lower water imbibition compared to the other reference samples. Two factors influence the anomaly behavior of this particular sample: firstly, the measurement may be dissimilar during imbibition due to the presence of

undissolved salt in pore volume diluted during water imbibition thus, a more substantial path is accessible to be occupied by water. Secondly, the measurement of porosity is also influenced by the presence of trapped air, which results in incomplete nitrogen invading the pore structure.

Crude imbibition and water imbibition comparison

The porosity of the rock sample is determined using the crude oil imbibition, in which the samples are saturated with crude oil at (41) API degrees and a density of (0.82 gm/cm³). The dry weight is measured again after 24 hours of vacuum drying at (50 °C) and the finding is shown below:

It is obvious that some samples due to their fragile nature, developed fractures and fragments, resulting in decreased dry weight measurements.

Porosity measurements of the nine irregular samples entailed introducing them into the vacuum chamber four times to obtain the porosity. For the water imbibition, each trial took (5 minutes). So, for each sample, in total it takes around (20 minutes) under vacuum conditions to reach a compatible preceding reading with the crude oil imbibition, each trial takes (10 minutes), therefore, each sample takes around (40 minutes) to attain full saturation. The difference in vacuum time required between the oil and water imbibition is due to the fact that the oil is more viscous than water, causing to flow under slower rate. Another factor contributing to the measurement is the wettability, for instance, hydrophilic samples allow water to easily infiltrate through the pores due to its strong affinity for water. Contrarily, the crude oil may find greater resistance in hydrophilic samples. The porosity is calculated using the same equations as the water saturation approach, and the results are shown in [Table 5](#). For example, S6 shows a significant difference between

both measurements and records higher readings in the water imbibition trail, and that indicates the sample is strong-water wet as the water has higher surface tension leading to higher capillary pressure that forces the water into pores. Moreover, the viscous crude is not able to flow easily. In the meantime, there is minimal variation between samples S8, S9, S11, and S14. This may be identified due to weak pore connectivity, in the presence of isolated pores, fluid may be unlikely to get through the pores, hence pore size distribution (micro to macro) exhibits varied porosity measurements. S12 with a higher pore volume compared to the previous samples showed similar behavior for both of the fluids with slight variation and is considered neutral wettability. The presence of organic matter or a hydrophobic mineral may alter the affinity slightly towards the crude oil. Both S7 and S13 tend to adsorb crude oil more than other readings though the reading is close to both imbibition. It is interpreted as the presence of mixed wettability and slightly higher in the hydrophobic region that may be caused by the temperature fluctuation between days and night and different seasons. Moreover, the mineral interaction with the fluid as the clay swells in contact with water leads to lower porosity readings. The sample's wettability preference will be evident from fluid saturation changes and worth mentioning that wettability does not influence the rocks' genuine porosity. However, it has a substantial impact on how fluids behave within the pore spaces, affecting fluid flow and, ultimately oil recovery.

Crude oil weight (g):

$$W_{Crude\ oil} = W_{saturated} - W_{dry} \quad \dots (9)$$

$$\text{Pore volume (cc): } V_p = \frac{W_{Crude\ oil}}{\rho_{Crude\ oil}} \quad \dots (10)$$

Table 5: Comparison between water imbibition method and crude imbibition method.

Sample	V _{B2} *	Dry weight 2*	Last saturated weight 2*	Crude oil Porosity %*	Porosity H ₂ O %	Difference
S6	43	108.61	109.83	3.46	9.89	6.43
S7	78	193.96	198.43	6.99	5.53	1.46
S8	125	322.97	325.82	2.78	2.67	0.11
S9	170	425.02	427.74	1.95	2.50	0.55
S10	123.5	332.68	333.89	1.19	0.11	1.08
S11	109	289.15	289.76	0.68	0.28	0.40
S12	106	263.28	269.46	7.10	7.76	0.66
S13	91	217.28	224.24	9.30	5.46	3.84
S14	196	518.61	520.93	1.44	2.02	0.58

CONCLUSION

- Applicability of measuring porosity from imbibition employed in this project is available and within reach for every researcher simple and time-conserving.
- Pearson correlation between nitrogen porosity and water imbibition provided a moderate result. The outcome of the correlation is compatible with the correlation tune in water imbibition results and provides a beneficial matching system for most of the samples.
- The percentage of porosities calculated from the outcrop samples might be slightly higher than the same core taken from the reservoir because the core plugs are more compacted and tighter than the outcrops.
- The difference between crude oil and water imbibition is attributed to the following: factors wettability, fluid properties (viscosity, interfacial tension), and rock structure. The sample will imbibe more of the fluid it's preferentially wet towards. For example, a higher oil saturation after oil imbibition indicates an oil-wet system.
- To conclude the water saturation measurement is beneficial for this set of data, however, more accurate results can be obtained when the mineral and pore structure are provided and core samples from reservoirs in a nonlinear correlation comparison for future research to raise the accuracy of the measurement.

Conflict of interests: The authors declared no conflicting interests.

Sources of funding: This research did not receive any specific grant from funding agencies in the public, commercial, or not-for-profit sectors.

Author contribution: Authors contributed equally in the study.

REFERENCES

1. Ahmed T. Reservoir engineering handbook: Gulf professional publishing; 2018.
2. Dandekar AY. Petroleum Reservoir Rock and Fluid Properties. CRC Press; 2013.
<https://doi.org/10.1201/b15255>
3. Anovitz LM, Cole DR. Characterization and analysis of porosity and pore structures. Reviews in Mineralogy and geochemistry. 2015;80(1):61-164.
<http://dx.doi.org/10.2138/rmg.2015.80.04>
4. PWJ G. Formation Evaluation MSc. Course Notes – Wettability, Chapter 7 September 2024.
5. Wei B, Liu J, Zhang X, Xiang H, Zou P, Cao J, et al. Nuclear Magnetic Resonance (NMR) mapping of remaining oil distribution during sequential rate waterflooding processes for improving oil recovery. Journal of Petroleum Science and Engineering. 2020;190:107102.
<https://doi.org/10.1016/j.petrol.2020.107102>
6. Grader A, Kalam M, Toelke J, Mu Y, Derzhi N, Baldwin C, et al. A comparative study of digital rock physics and laboratory SCAL evaluations of carbonate cores. SCA2010-24 Nova Scotia. 2010.
7. Kazimierz T, Jacek T, Stanislaw R. Evaluation of rock porosity measurement accuracy with a helium porosimeter. Acta Montanistica Slovaca. 2004;3:316-8.

8. Ogolo NA, Akinboro OG, Inam JE, Akpokere FE, Onyekonwu MO, editors. Effect of grain size on porosity revisited. SPE Nigeria annual international conference and exhibition; 2015: SPE. <https://doi.org/10.2118/178296-MS>
9. Kazatchenko E, Mousatov A, editors. Primary and secondary porosity estimation of carbonate formations using total porosity and the formation factor. SPE Annual Technical Conference and Exhibition?; 2002: SPE. <https://doi.org/10.2118/77787-MS>
10. Kułynycz V. The influence of wettability on the petrophysical parameters of reservoir rocks. AGH Drilling, Oil, Gas. 2017;34(3). <http://dx.doi.org/10.7494/drill.2017.34.3.775>
11. Eppes M, Magi B, Scheff J, Warren K, Ching S, Feng T. Warmer, wetter climates accelerate mechanical weathering in field data, independent of stress-loading. Geophysical Research Letters. 2020;47(24):2020GL089062. <https://doi.org/10.1029/2020GL089062>
12. Kim JH, Ree J-H, Tanikawa W, Kang H-C. The effect of weathering on cohesion in granitic fault rocks: A case study from the Yeongdeok Fault, South Korea. Journal of Structural Geology. 2024;179:105061. <https://doi.org/10.1016/j.jsg.2024.105061>
13. Bachmann J, Söffker S, Sepehrnia N, Goebel MO, Woche SK. The effect of temperature and wetting–drying cycles on soil wettability: Dynamic molecular restructuring processes at the solid–water–air interface. European Journal of Soil Science. 2021;72(5):2180-98. <https://doi.org/10.1111/ejss.13102>
14. Garfi G, John CM, Lin Q, Berg S, Krevor S. Fluid surface coverage showing the controls of rock mineralogy on the wetting state. Geophysical Research Letters. 2020;47(8):e2019GL086380. <https://doi.org/10.1029/2019GL086380c>
15. Kumar S, Burukhin AA, Cheremisin AN, Grishin PA, editors. Wettability of carbonate reservoirs: effects of fluid and aging. SPE Russian Petroleum Technology Conference?; 2020: SPE. <https://doi.org/10.2118/201834-MS>
16. Mousavi S-P, Hemmati-Sarapardeh A, Norouzi-Apourvari S, Jalalvand M, Schaffie M, Ranjbar M. Toward mechanistic understanding of wettability alteration in calcite and dolomite rocks: The effects of resin, asphaltene, anionic surfactant, and hydrophilic nano particles. Journal of Molecular Liquids. 2021;321:114672. <https://doi.org/10.1016/j.molliq.2020.114672>
17. Cao N, Almojtaba Mohammed M, Babadagli T. Wettability alteration of heavy-oil-bitumen-containing carbonates by use of solvents, high-pH solutions, and nano/ionic liquids. SPE Reservoir Evaluation & Engineering. 2017;20(02):363-71. <https://doi.org/10.2118/183646-PA>
18. Harraz H. Z. Porosity measurement. 2019.
19. Schmoker KBKaRBHJW. Selected characteristics of limestone and dolomite reservoirs in the United States. American Association of Petroleum Geologists,. 1985;69(5):733-41.
20. S. Turner Vc. CERN EUROPEAN ORGANIZATION FOR NUCLEAR RESEARCH. Vacuum chamber. 1999.
21. Tian H, Zou C, Liu S, Hong F, Fan J, Gui L, et al. Reservoir porosity measurement uncertainty and its influence on shale gas resource assessment. Acta Geologica Sinica-English Edition. 2020;94(2):233-42. <https://doi.org/10.1111/1755-6724.14287>
22. Ahmed SH, editor Designation and study of anticlines-Kurdistan region-NE Iraq. Journal of Physics: Conference Series; 2019: IOP Publishing. <http://dx.doi.org/10.1088/1742-6596/1294/8/082001>
23. Sarraj RH, Mohialdeen IM, Kalaitzidis S. Organic petrographical features and thermal maturity assessment of the Cretaceous Balambo Formation from Zagros Fold-Thrust Belt, Kurdistan Region, Northern Iraq. Arabian Journal of Geosciences. 2021;14:1-11. <http://dx.doi.org/10.1007/s12517-020-06260-3>
24. Alavi M. Regional stratigraphy of the Zagros fold-thrust belt of Iran and its proforeland evolution.

- American journal of Science. 2004;304(1):1-20.
<http://dx.doi.org/10.2475/ajs.304.1.1>
25. Al-Juboury AIA. The upper Miocene Injana (upper Fars) formation of Iraq: Insights on provenance history. Arabian journal of geosciences. 2009;2:337-64.
<http://dx.doi.org/10.1007/s12517-009-0045-1>
26. Qader FM, Ali SM. Reservoir Characteristics of the Lower Miocene Carbonate Formations in Kor Mor Gasfield, Kirkuk Area, NE Iraq. Tikrit Journal of Pure Science. 2022;27(3):43-52.
<http://dx.doi.org/10.25130/tjps.27.2022.037>
27. Buday T. The regional geology of Iraq: tectonism, magmatism and metamorphism: State Organization for Minerals, Directorate General for Geological Survey ...; 1980.
28. Al-Talabani MJA. Stratigraphic study of Qalqula Formation, Sulaymaniyah Governorate-NE Iraq. Tikrit Journal of Pure Science. 2018;23(10):60-5.
<https://doi.org/10.25130/tjps.v23i10.564>
29. Jassim SZ, Goff JC. Geology of Iraq: DOLIN, sro, distributed by Geological Society of London; 2006.
30. Rasheed H.J.M. Petroleum system in 'Kurdistan (North Iraq). Global Scientific Journals. 2020;8(4):213-9.
31. Al-Qayim B, Ghafor I, Jaff R. Contribution to the stratigraphy of the Walash Group, Sulaimani area, Kurdistan, Iraq. Arabian Journal of Geosciences. 2014;7:181-92.
<https://doi.org/10.1007/s12517-012-0809-x>
32. Washburn EW, Bunting EN. Porosity: VI. Determination of porosity by the method of gas expansion. Journal of the American Ceramic Society. 1922;5(2):112-30.
<https://doi.org/10.1111/j.1151-2916.1922.tb17640.x>
33. ASTM D. 4404; Standard Test Method for Determination of Pore Volume and Pore Volume Distribution of Soil and Rock by Mercury Intrusion Porosimetry. ASTM Standards: West Conshohocken, PA, USA. 2018.
34. Davis LA, Moss RM, Pepin GP. Direct measurement of the constituent porosities in a dual-porosity matrix. The Log Analyst. 1992;33(02).
35. Schober P, Boer C, Schwarte LA. Correlation coefficients: appropriate use and interpretation. Anesthesia & analgesia. 2018;126(5):1763-8.
<https://doi.org/10.1213/ANE.0000000000002864>